RAA 2020 Vol. **20** No. **3**, 30(12pp) doi: 10.1088/1674–4527/20/3/30

http://www.raa-journal.org *http://iopscience.iop.org/raa*

Research in Astronomy and Astrophysics

Stray light analysis of the Xinglong 2.16-m telescope

Tao-Ran Li[1], Jian-Feng Wang[1], Xiao-Ming Zhang[1], Yong Zhao[1,2] and Jian-Feng Tian[1]

[1] Key Laboratory of Optical Astronomy, National Astronomical Observatories, Chinese Academy of Sciences, Beijing 100101, China; *litaoran@bao.ac.cn*

[2] University of Chinese Academy of Sciences, Beijing 100049, China

Received 2019 July 4; accepted 2019 September 24

Abstract An effort towards understanding the problems associated with stray light related to the Xinglong 2.16-m telescope is presented to estimate the stray light performance of the telescope itself and provide a method for improving stray light suppression. Stray light analysis for the 2.16-m telescope model, which consists of an onion shaped dome, telescope structure, equatorial mount and telescope optics, has been developed in two cases (1) pointing to 60° and (2) pointing to zenith, in both azimuth and elevation directions. The Point Source Normalized Irradiance Transmittance (PSNIT), which is generally used for assessing stray light and is uncorrelated to entrance aperture, is calculated with a series of off-axis angles. It shows that the PSNIT values are less than 10^{-7} when off-axis angles are larger than $\pm 20°$. The dominant contributors to stray light (primary and secondary mirror, telescope structure and dome) are identified to guide performance improvement. The analyses indicate that significant benefit can be realized by adding only five vanes inside the bottom portion of the secondary baffle. In the case of pointing to zenith, the PSNIT values will decrease about 40% on average.

Key words: telescope — scattering — methods: data analysis

1 INTRODUCTION

The Xinglong 2.16-m telescope, inaugurated into service in 1989 and located at the Xinglong Observatory, is a Ritchey-Chrétien telescope, with a primary mirror of diameter 2.16 meters (Fan et al. 2016). The optical system of this 2.16-m telescope is presented in Figure 1. The hyperboloidal primary mirror (M1) and convex secondary mirror (M2) make the effective focal length for the Cassegrain focus 19.4 m (f/9) (Su 2001). As displayed in Figure 2, the 2.16-m telescope has a conventional open truss form design and an equatorial-type mount. The initial opto-mechanical design comprises two baffles, which are the M2 baffle surrounding the secondary mirror M2 and the primary baffle above the primary mirror M1.

During observations performed over 30 years, a few baffling solutions (vanes on the inner surface of the primary baffle) and some tests have been made, but the stray light performance of the telescope remains unknown, which is critical for high-performance of the optical instruments. Sometimes, unidentified scattered light could be seen on the detector during a bright night.

This paper describes efforts towards understanding the stray light problems with the telescope itself without the instruments. The stray light analysis is aimed at estimating the stray light performance of the 2.16-m telescope and provides an overview of the stray light suppression for future instruments (e.g., a new intermediate-resolution spectrograph and tip-tilt module). The software SOLIDWORKS, TracePro and MATLAB is employed for modeling, ray tracing and analyzing, respectively

The paper is organized as follows: Section 2 introduces the stray light model of the 2.16-m telescope, definition of Point Source Normalized Irradiance Transmittance (PSNIT) and simulation settings. Identification of critical objects and illuminated objects are described in Section 3. The analyses of PSNIT curves and stray light contributors in two cases are presented in Sections 4 and 5 respectively. Finally, a brief conclusion is discussed in Section 6.

2 STRAY LIGHT MODEL OF XINGLONG 2.16-M TELESCOPE

Stray light is generally defined as unwanted light that reaches the focal plane of an optical system (Bass et al. 2001). It is one of the most important factors that influence high-accuracy photometry of optical astronomical telescopes, which could reduce the signal to noise ratio

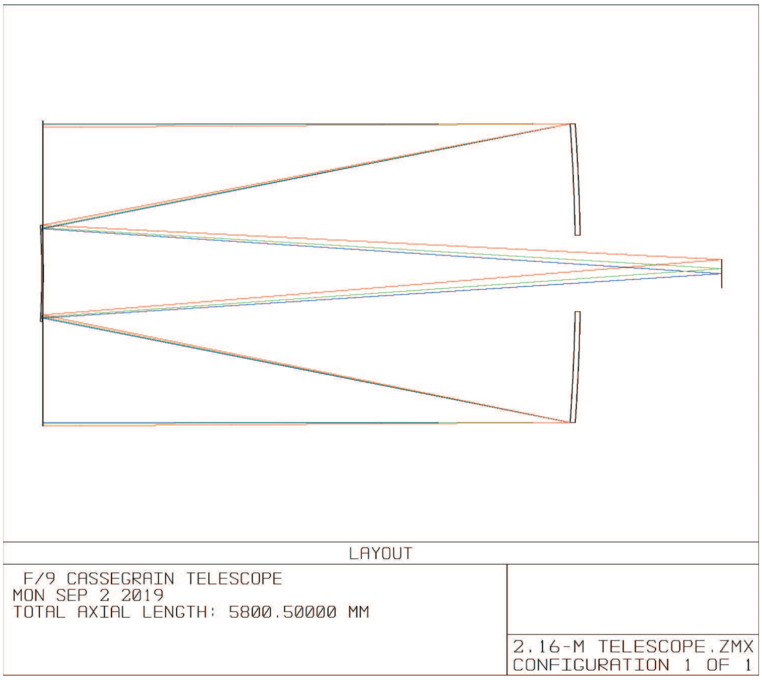

Fig. 1 Optical layout of the Xinglong 2.16-m telescope's f/9 Cassegrain focus. The diameter of the primary mirror is 2.16-m. *Red rays* are from an axis point source at infinity. *Blue* and *green rays* are from a source with radius 6 arcmin and 18 arcmin, respectively.

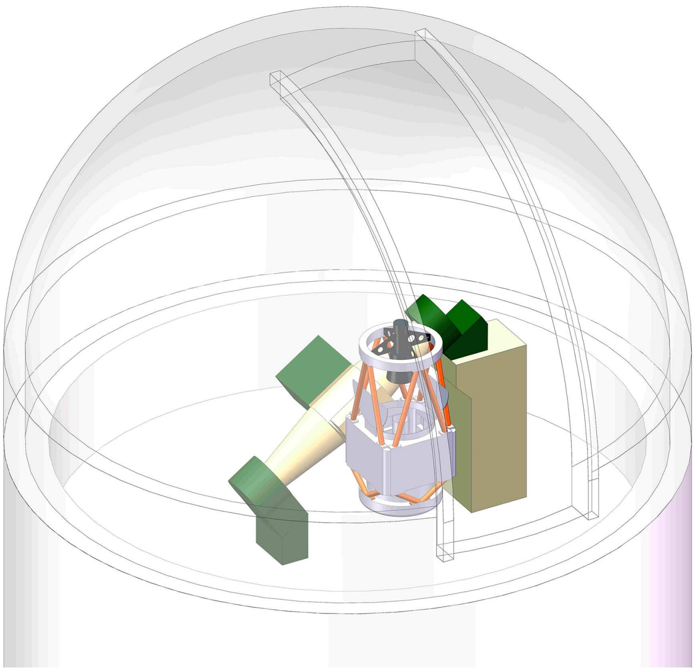

Fig. 2 SOLIDWORKS model of the Xinglong 2.16-m telescope, including the enclosure (rotating dome with slit, in transparent), equatorial mount (south and north pier, in emerald green and dark green respectively), mirror cell, Serrurier truss, top-end ring, cylindrical baffles for the primary (M1) and secondary (M2) mirrors, and vanes on the inner surface primary baffle.

of astronomical objects. Stray light analysis begins with the 3D modeling of the optical and mechanical geometry. Then, ray tracing is applied with the associated simulation parameter settings and the surface properties in ray tracing software (TracePro).

2.1 Telescope and Dome Simplification

The original model contains tiny parts and complex shapes which can increase simulation time and are not necessary. Therefore, the mechanical model should be simplified (e.g., removing the screws and reconstructing the top end assembly as an annular part).

The simplified TracePro model has eight basic components:
(1) Dome
(2) Mount
(3) Telescope structure (spider, top end assembly, truss, center section, Cassegrain focus interface)
(4) Secondary baffle
(5) Primary baffle
(6) Vanes (on the inner surface of the primary baffle)
(7) Optical system
(8) CCD

The 2.16-m telescope has an onion shaped dome with a 22 meter internal diameter and an up-and-over shutter (5200 mm wide). The distance between the top of the slit and the top end of the telescope is about 8700 mm. The inner diameters of the primary and secondary baffle are 574 mm and 960 mm respectively. Sketching additional rays representing how moonlight varies with azimuth indicate that the scattered light will be blocked from directly reaching (1) the primary baffle by the edge of secondary baffle, and (2) the M1 by the edge of secondary baffle and dome slit, if the angular distance from the Moon is less than $\pm 7.1^\circ$ and larger than $\pm 13.2^\circ$, respectively (positive: right side of the dome slit). As in elevation, the moonlight will be will be blocked by (1) the edge of dome slit and secondary baffle, and (2) center section, if the Moon's distance is larger than +14.6° and –95.6°, respectively (positive: left side of the telescope), as displayed in Figure 3.

2.2 Stray Light Calculation Method

PSNIT is a transfer function which describes the stray light performance in an optical system, equal to the average irradiance over the focal plane divided by the incident irradiance at the instrument (Fest 2013). PSNIT is one of the types of Point Source Transmittance (PST), implemented in some systems such that the entrance aperture may not be well defined. Due to the open-truss structure used with the 2.16-m telescope, it is hard to define the entrance aperture. Here the PSNIT is calculated by

$$\begin{aligned} \mathrm{PSNIT} &= \frac{E_{\mathrm{focal-plane}}}{E_{\mathrm{incident}}} \\ &= \frac{P_{\mathrm{focal-plane}}/\mathrm{area}_{\mathrm{focal-plane}}}{P_{\mathrm{incident}}/\mathrm{area}_{\mathrm{incident}}}\,, \end{aligned} \tag{1}$$

where E is the irradiance defined as the total power P per area. The irradiance of an incident source is set to $1\,\mathrm{W\,m^{-2}}$ and the area of the focal plane is $30\,\mathrm{mm}\times 30\,\mathrm{mm}$. Therefore, PSNIT is relevant only to the power on the focal plane.

2.3 Source Settings

Stray light sources are generally viewed as point sources. The light sources for simulation are dependent on the off-axis angle of the Moon. The illumination area of each source should be large enough to cover the whole dome shutter, which is the only path for moonlight entering the dome. The sources included in azimuth direction and elevation direction simulations are perpendicular and parallel to the direction of the shutter, respectively (Fig. 4). The stray light sources in both azimuth and elevation range from 0° to $\pm 90^\circ$. Each source has one million rays. The source beam has a uniform spatial and angular profile, entering the system randomly.

2.4 Surface Property

Bidirectional Scattering Distribution Function (BSDF) is a common method employed to describe the scattering characteristics of a surface. Bidirectional Reflectance Distribution Function (BRDF) and Bidirectional Transmittance Distribution Function (BTDF) are subclasses of BSDF, used to describe the reflectance and transmittance, respectively (Bartell et al. 1981). The BSDF measures both the incident and scattering directions. Mathematically, the BSDF is defined as scattered radiance per unit incident irradiance (TracePro 2010)

$$BSDF(\theta_i, \phi_i, \theta_s, \phi_s,) = \frac{dL_s(\theta_s, \phi_s)}{dI_i(\theta_i, \phi_i)}. \tag{2}$$

Here θ and ϕ are angles in spherical coordinates, i and s subscripts refer to incident and scattered cases respectively, and L and I are radiance and irradiance, respectively. The unit of radiance here is $\mathrm{W\,m^{-2}\,sr^{-1}}$ and that for irradiance is $\mathrm{W\,m^{-2}}$.

The BSDF is a function of many parameters and normally it is difficult to develop highly accurate theoretical models. However, due to the time and budget required, the precise surface properties are hard to measure. Fortunately, there are many surface properties available both empirically and theoretically in TracePro. These include absorptance, specular reflectance, transmittance, BRDF and BTDF. As the specular reflectance is easy to obtain, the optical elements (M1 and M2) implement the default mirror model in the database, with no dust on the optical surface, and just modify the specular reflectance as the measured value. The other surfaces are treated as "black paint" to absorb the stray light as much as possible. Table 1 lists the surfaces and their parameters.

2.5 Importance Sampling

Importance sampling is a technique employed in Monte Carlo calculations to improve efficiency (Greynolds 2007).

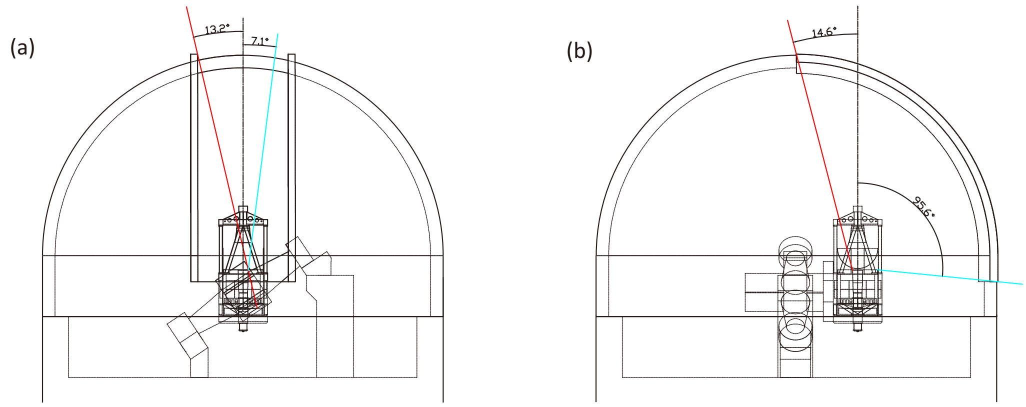

Fig. 3 Layout of dome and simplified 2.16-m telescope components in profile view, with some limiting lines of sight from the Moon to different points on the telescope structure. (a) Stray light source that varies with azimuth, a view through the dome slit, demonstrating that light from the Moon cannot enter the M1 baffle when the Moon's angular distance from the telescope is less than 7.1° (*blue line*, blocked by the M2 baffle) or larger than 13.2° (*red line*, blocked by edge of dome slit); (b) Stray light source that varies with elevation, and a view with the dome rotated by 90°, dome slit at right, showing that light from the Moon cannot enter the M1 baffle if the Moon's zenith distance is more than 14.6° in the direction away from the dome slit (*red line*, blocked by edge of the dome slit) and it cannot impinge on M1 directly if the zenith distance is more than 95.6° (*blue line*, blocked by the telescope's center section).

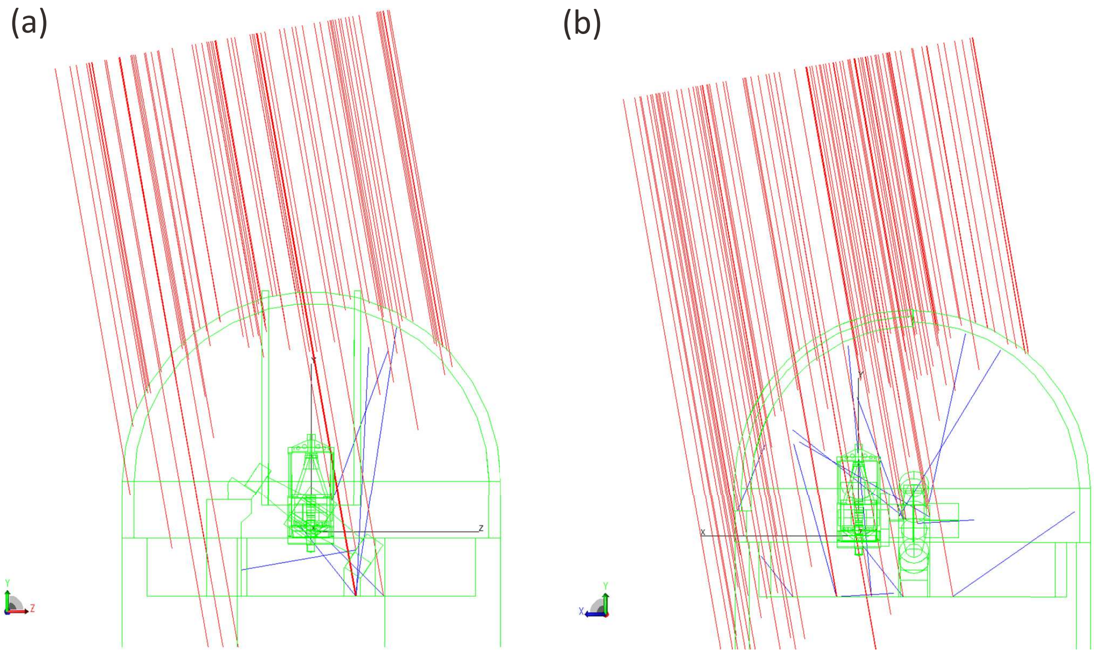

Fig. 4 Azimuth and elevation simulation (in TracePro) of light from a point source at infinity, impinging on the dome, telescope and support structure. The telescope is pointed to zenith. *Left*: azimuth; *right*: elevation. These only for illustrate the location of the sources, and are not the same as the following simulation.

Table 1 Surface Property Parameters In TracePro

	Surface	Property
1	Mirror surface of M1 and M2	Absorptance: 9.9%, Specular reflectance: 90.0%, Integrated BRDF: 0.1%
2	Other surfaces	Absorptance: 90.0%, Specular reflectance: 2.0%, Integrated BRDF: 8.0%
3	Outside surfaces of the dome	Perfect absorber-Absorptance: 100.0%

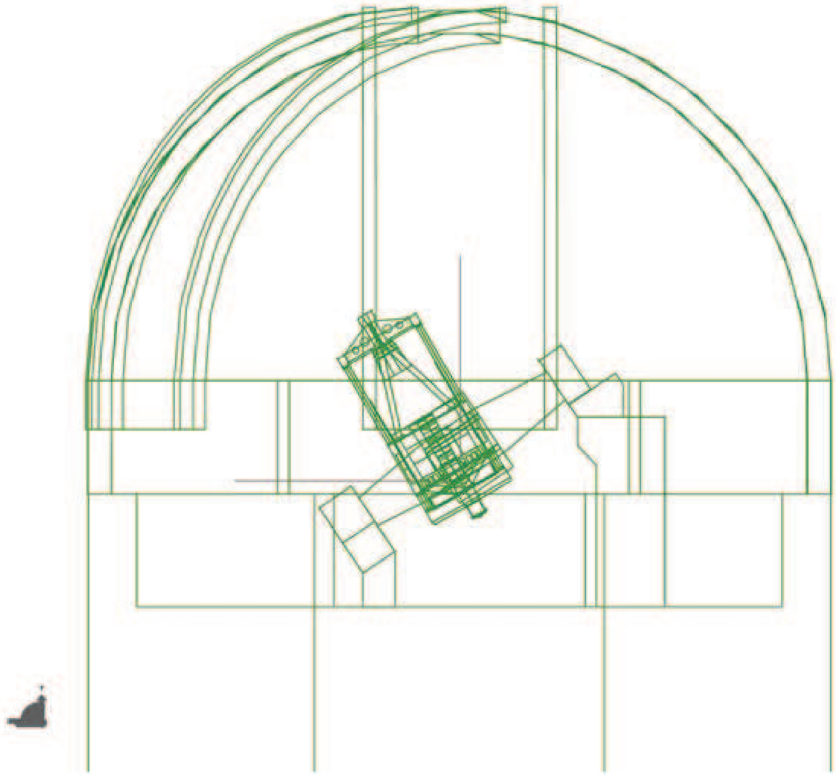

Fig. 5 Model of telescope pointing to 60° in elevation. Due to the equatorial mount, the dome shutter is collinear with the telescope.

The "important" surfaces are forced to occur with higher probability than their nature. The stray light model with importance sampling could avoid relying on millions of rays and perform the ray tracing in a reasonable time. An "importance" surface should have one or more targets where the rays are supposed to go, either toward or away from the "importance" surface. In stray light simulation, the importance sampling should be selected on each first-order scattering surfaces.

3 CRITICAL AND ILLUMINATED SURFACES

The first step in ray tracing is to identify the critical and illuminated surfaces. A critical surface is one that can be seen by the detector directly or indirectly through mirror reflection. Most optical surfaces in the telescope are critical surfaces. An illuminated surface is one that is illuminated by a stray light source directly or indirectly through mirror reflection (Schaub et al. 2011).

The first-order stray light path always occurs on the first-order scattering surfaces which are both critical and illuminated. The first-order paths are the primary propagation paths for stray light (Bely 2003). In order to identify the critical and illuminated surfaces, backward ray tracing from the detector and initial ray tracing from the stray light source should be made.

The basic idea involved in critical surface identification is to (1) analyze the system from the detector, (2) check the ray tracing history of every surface and (3) find the surfaces visible from the detector. The initial ray tracing from a stray light source is similar to the backward ray tracing. It utilizes several sources with different off-axis angles to find the surfaces which are illuminated directly. The critical and illuminated surfaces include the following:

Critical surfaces:

1 Cassegrain focus interface: inner surfaces
2 Center section: inner surfaces
3 M1: mirror surface
4 M2: mirror surface
5 Primary baffle: inner surface and upper edge
6 Secondary baffle: inner surface and bottom edge
7 Vanes: knife surfaces, upper and bottom surfaces

Illumination surfaces:

1 Primary baffle: inner surface, outside surface and upper edge
2 Secondary baffle: inner surface, outside surface and bottom edge

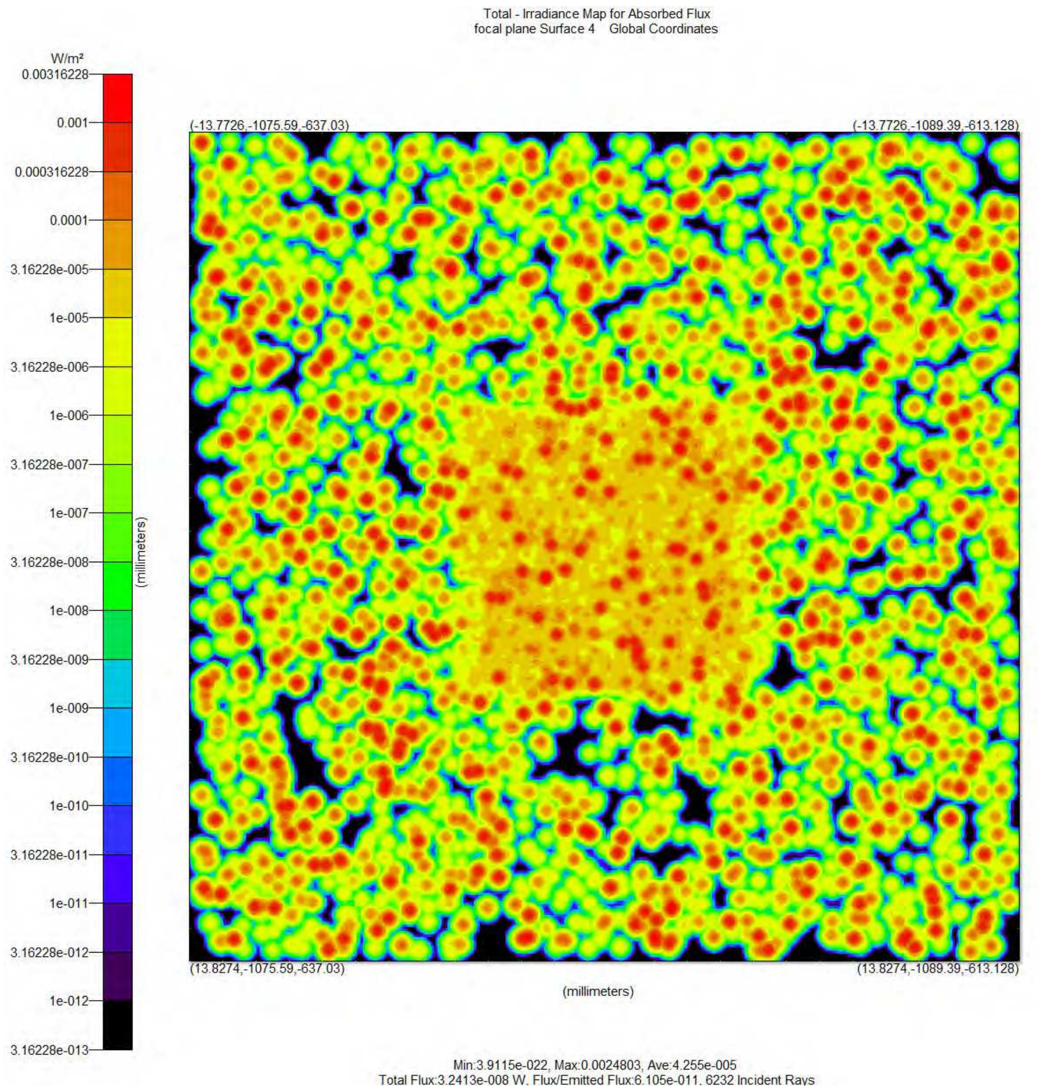

Fig. 6 Irradiance map (predicted distribution of stray light) on focal plane for azimuth angle$=5^\circ$, in watts per area. Most of the stray light is located in a box due to the importance sampling.

3 M1: mirror surface
4 M2: mirror surface
5 Vanes: knife surfaces and upper surfaces
6 Center section: inner surfaces
7 Other telescope structures (spider, top end assembly, truss)
8 Dome surfaces

The first-order scattering surfaces and their importance sampling targets are displayed in Table 2.

4 STRAY LIGHT ANALYSIS OF CASE 1: TELESCOPE IS POINTED TO 60°

The first attempt is pointing the telescope to 60° in elevation, as depicted in Figure 5. The dome slit is collinear with the telescope. An irradiance map (Fig. 6) displays the distribution and intensity of stray light on the focal plane. Most of the stray light is located in a rectangular box on the focal plane due to the importance sampling. The total power in Equation (1) is derived from the total flux in the irradiance map when simulations of each angle are finished. Figure 7 features plots of the PSNIT curves for azimuth (red line) and elevation (blue line) with logarithmic coordinates. The labels on the two plots illustrate the most significant contributors to the stray light flux at each angle. This is done by "*Ray Path Sorting*" in TracePro (Table 3). The label "*Tel.structure*" includes the mount, spider, top end assembly, truss, center section and other parts of the structure of the telescope.

4.1 Stray Light Analysis in Azimuth Direction

In the azimuth simulation, positive angles are located at the right side of the dome shutter ($+Z$ direction in Fig. 4 left). For the angles between the edge of the field of view

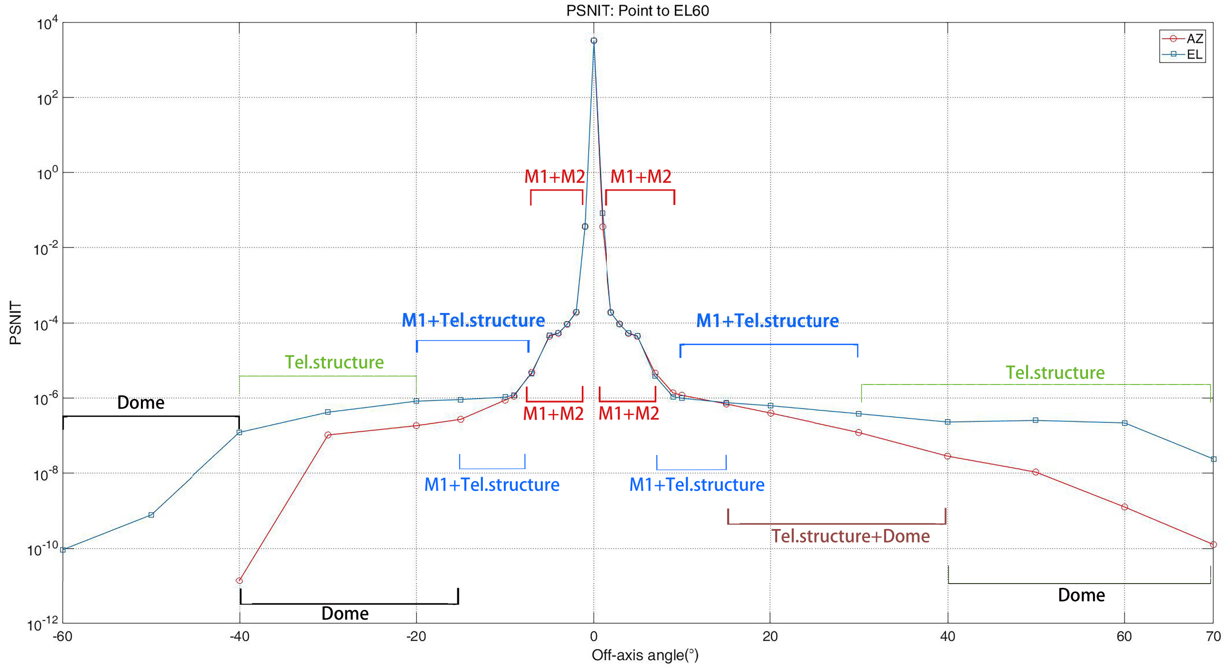

Fig. 7 PSNIT curve for azimuth and elevation, where the telescope is pointed to 60°. Predicted relative intensity (PSNIT - see Sect. 2.2) of scattered moonlight, as a function of angular distance from the Moon in elevation (*blue*) and azimuth (*red*). The dominant sources of scattered light are indicated by the labels above (for the elevation curve) and below (for the azimuth curve) the plotted curves; e.g., 'M1+M2' means that a large fraction of scattered light arises from moonlight arriving directly on M1 but scattered up to M2 and then scattered down through the Cassegrain hole to the focal plane. The dramatic drops in scattered light intensity at azimuth beyond ±7° are due to the secondary baffle blocking moonlight (see Fig. 3). The *blue line* stops at –40° because no scattered light arrives on the focal plane at azimuth angles larger than –40°.

Table 2 The First-order Scattering Surfaces and the Importance Sampling Targets

	First-order scattering surface	Importance sampling target
1	M1: mirror surface	Primary focus
2	M2: mirror surface	Focal plane
3	Primary baffle: inner surface and upper edge	Focal plane+image of focal plane produced by M2
4	Secondary baffle: inner surface and bottom edge	Focal plane
5	Center section: inner surfaces	Image of focal plane produced by M2
6	Vanes: knife surfaces and upper surfaces	Image of focal plane produced by M2

Table 3 Type of Ray Path for 10° (Percentage $>$ 3%)

Ray Path	No. of Rays	% of Total	Path Type	Object
1	1618	42.49	Single Scatter	Source-M1-M2-focal plane
2	11	7.23	Multiple Scatter	Source-Center section-Secondary baffle-focal plane
3	16	4.34	Multiple Scatter	Source-Mount-Secondary baffle-focal plane
4	128	3.41	Multiple Scatter	Source-Dome-M1-M2-focal plane

(FOV) and ±10°, the PSNIT curve is nearly symmetrical with respect to the Y axis. The specular rays reflected by M1 and M2 dominate the stray light at off-axis angles less than ±7°. The dramatic drops in scattered light intensity at azimuth beyond ±7° are due to blocking of moonlight by the secondary baffle. The structure of the telescope is another contributor for angles between ±7° and ±15°, and the rays can directly illuminate the outside surface of the center section and the mount, then randomly scatter into the secondary baffle. M1 is not the contributor after ±15°, at which point the rays entering the dome shutter no longer directly illuminate M1 (Fig. 8 left). Beyond ±15°, the rays are gradually blocked by the dome, and the telescope structure and inner surface of the dome become the primary

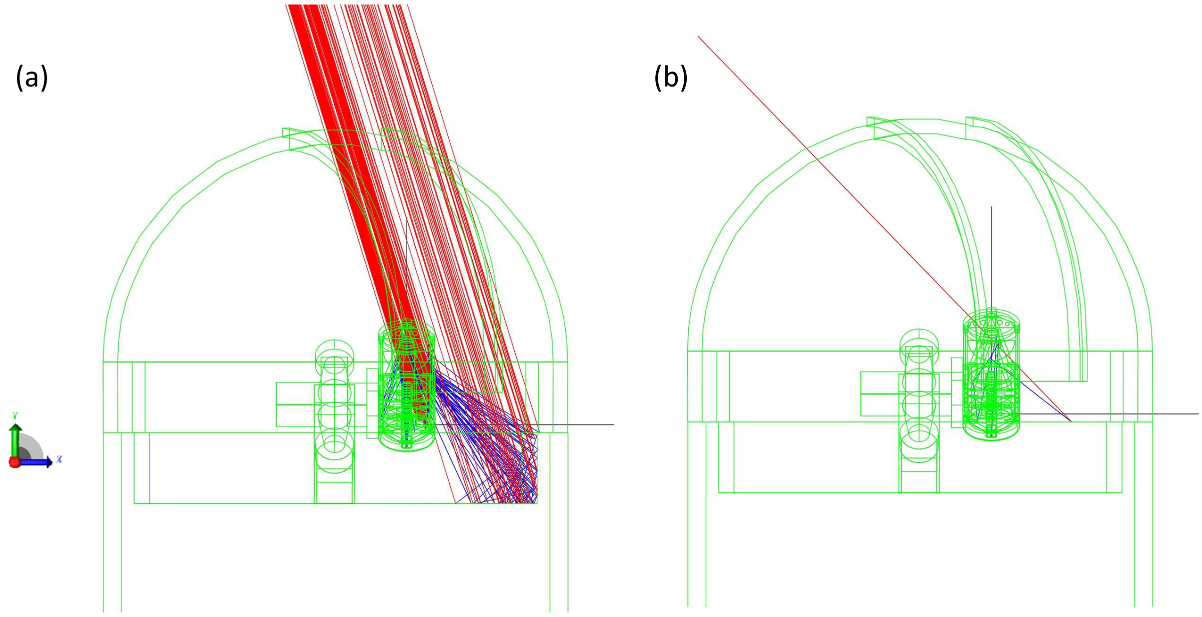

Fig. 8 Ray tracing at –15° (a) and –40° (b) in the azimuth simulation.

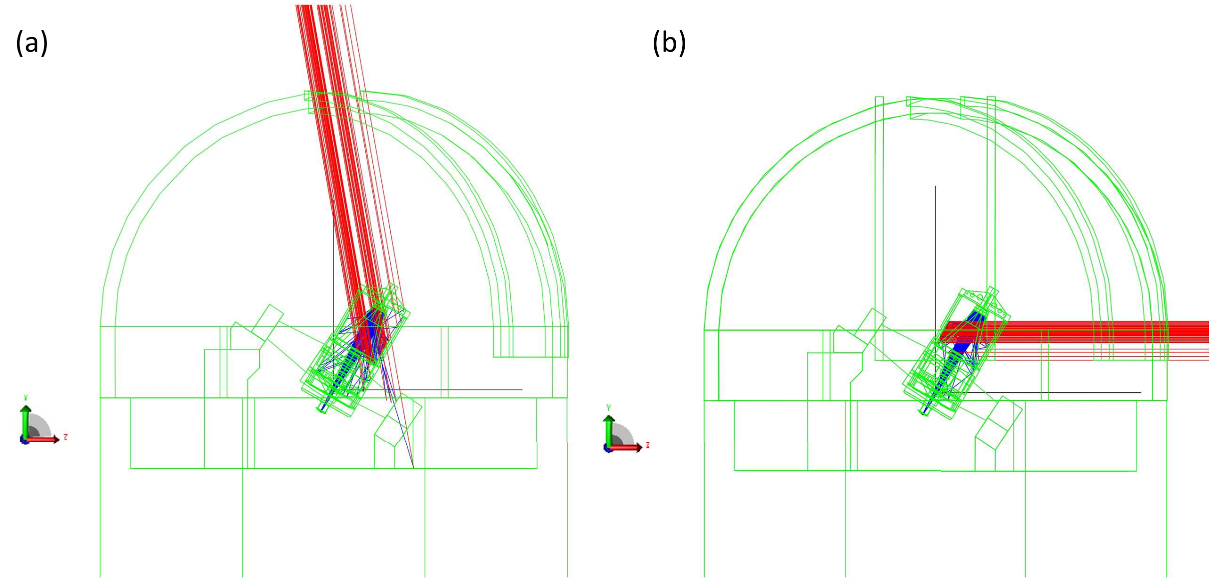

Fig. 9 Ray tracing at +60° (a) and –40° (b) in the elevation simulation.

contributors. As the source angle increases, the rays entering the dome move higher up the dome walls. For input angles greater than +40°, the inner surfaces of the dome are the most significant contributors.

Due to the English mount of the 2.16-m telescope, the whole model is asymmetric. The PSNIT curve stops at –40° because no light is scattered on the focal plane at azimuth angles larger than –40°. The PSNIT value is less than 10^{-7} when the off-axis angle is larger than $\pm 20°$. The minimum PSNIT is 1.4×10^{-11}, at which angle (–40°) only one ray is scattered on the focal plane by random scattering from the dome surface.

4.2 Stray Light Analysis in Elevation Direction

In elevation simulation, the positive angles are defined as the sources lower than the optical axis of the telescope. For the angles between 0° and $\pm 10°$, the PSNIT curves and the contributors of azimuth and elevation are almost the same. It is clear that the PSNIT values of elevation are larger than those of the azimuth after $\pm 15°$, because of scattering from the telescope structure.

In the positive direction, no part of the dome will block stray light from illuminating the telescope. M1 and telescope structure are the dominant sources from +15°

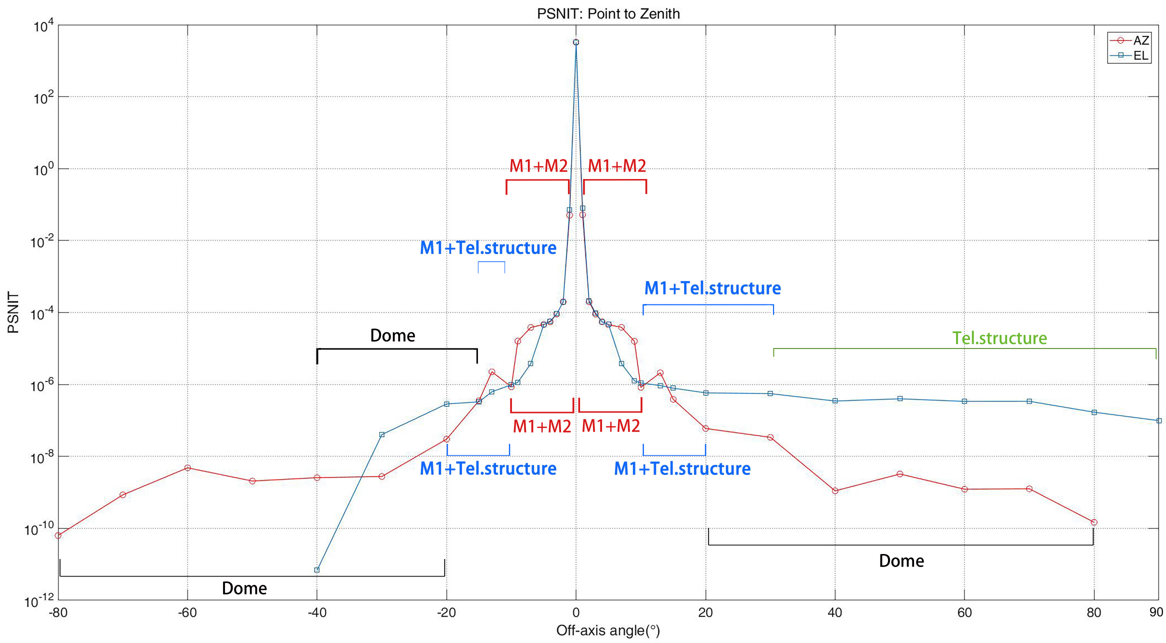

Fig. 10 Like Fig. 7, PSNIT curve for azimuth and elevation, when telescope is pointed to zenith.

to +30°. For elevation angles larger than +30°, the lights reflected from M1 no longer reach the M2 mirror cell, so the telescope structure is the only contributor. The PSNIT curve drops gradually as the elevation angles fall toward the horizon (the off-axis angle=60°), as illustrated in Figure 9(a).

For the curve along the negative direction, it is almost symmetrical with respect to the positive axis until the dome blocks the rays entering the telescope around –40° (Fig.9(b)), so the dome walls deliver more scattered lights.

4.3 Stray Light Distribution on Focal Plane

TracePro software will consume almost all the computer memory when running a simulation. It is better to archive results from several simulations rather than one-time ray tracing. Therefore, the stray light distribution can be analyzed roughly by combining all the results at different angles.

Table 4 provides the numbers of rays and fluxes on the focal plane in two axes of azimuth (0° to ±40°) and elevation (0° to ±40°). For the azimuth direction, the number of rays has a similar value on both sides of 0°, as well as the total flux. In the positive axis of elevation, the flux is larger than that along the negative axis because of no dome blocking.

Table 4 Number of Rays and Associated Flux on Focal Plane

	Azimuth		Elevation	
	Number of Rays	Flux	Number of Rays	Flux
Positive axis	59 628	2.64e-05	60787	6.08e-05
Negative axis	57 589	2.70e-05	62244	2.64e-05
Total	117 217	5.34e-05	123031	8.72e-05

Table 5 Number of Rays with or without Vanes

Off-axis angle	no vane-AZ	vane-AZ	no vane-EL	vane-EL
1	14684	13443	14604	11420
2	15631	13348	15650	11478
3	12499	10936	11098	9569
4	8766	7311	7430	6115
5	7593	6210	6438	5176
10	1974	1857	2244	2106
20	66	32	1300	1195
30	24	18	584	406
40	5	2	258	142
50	6	4	252	168
60	3	2	223	153
70	3	1	189	124
80	1	5	127	90
90	-	-	66	38
Total	61255	53169	60463	48180

5 STRAY LIGHT ANALYSIS OF CASE 2: TELESCOPE IS POINTED TO ZENITH

Another attempt is pointing the telescope to zenith. In this case, the system is approximately symmetrical in the azimuth direction. The max azimuth and elevation angles are 80° and 90°, respectively, as depicted in Figure 10.

Ray Path Sorting [216-elevation-importance sampling-bk]

Ray Path	Source	No. Rays	% of Total	Incident Flux	Path Type	No.	Intercept Type	Object	Surface
⊖ 1	30	31	9.95	4.02260723948443e-011	Single Surf Scat				
						1	Emitted		
						2	SpecRefl	center section	Surface 5
						3	SpecRefl	M2	Surface 0
						4	ImpRefl	M2 baffle	Surface 0
						5	At Surface	focal plane	Surface 4
⊖ 2	30	5	7.17	2.8990540311434e-011	Multiple Surf Scat				
						1	Emitted		
						2	RandRefl	center section	Surface 5
						3	ImpRefl	M2 baffle	Surface 0
						4	At Surface	focal plane	Surface 4
⊕ 3	30	18	5.89	2.38339688490314e-011	Single Surf Scat				
⊕ 4	30	4	5.60	2.26520429988391e-011	Multiple Surf Scat				
⊕ 5	30	15	5.22	2.11156743154354e-011	Single Surf Scat				
⊕ 6	30	15	5.17	2.09181920067334e-011	Single Surf Scat				
⊖ 7	30	11	3.37	1.36152906915244e-011	Single Surf Scat				
						1	Emitted		
						2	SpecRefl	M1	Surface 0
						3	SpecRefl	center section	Surface 11
						4	ImpRefl	M2 baffle	Surface 5
						5	At Surface	focal plane	Surface 4
⊖ 8	30	2	3.01	1.21725309923873e-011	Multiple Surf Scat				
						1	Emitted		
						2	RandRefl	mount	Surface 20
						3	ImpRefl	M2 baffle	Surface 5
						4	At Surface	focal plane	Surface 4
⊕ 9	30	2	2.91	1.17686675419417e-011	Multiple Surf Scat				

Fig. 11 The “Ray Path Sorting” table for elevation angle +30° of the case “point to zenith,” which provides the number of rays, flux percentage of each ray, incident flux, path type and ray path. “SpecRefl” means the specular reflection, “ImpRefl” refers to the importance sampling reflection/scattering and “RandRefl” signifies the random reflection/scattering.

5.1 Stray Light Analysis in Azimuth Direction

From the edge of the FOV to $\pm 10°$, the rays can reach the focal plane by M1 and M2 reflection or scattering. M1 and M2 are the primary contributors to stray light. The PSNIT curve drops very fast as the off-axis angle increases. No specular reflection by M1 happens at $\pm 10°$, where the PSNIT curve of azimuth has two steep drops. For angles between $\pm 10°$ and $\pm 20°$, the rays scattered by M1, together with the rays scattered by the structure of the telescope, dominate the total flux on the focal plane. As the stray light source is far away from the dome slit ($>20°$), the rays cannot illuminate the telescope directly, and the dome (by random scattering) becomes the primary contributor to stray light. Due to the multiple random scatterings by the dome, the curve is not smooth.

The PSNIT value is less than 10^{-8} when the off-axis angle is larger than $\pm 20°$. The minimum PSNIT is 6.32×10^{-11} at –80°. Compared with the azimuth PSNIT curve of the case “point to 60°,” the order of magnitude is similar to the case “point to zenith.”

5.2 Stray Light Analysis in Elevation Direction

The PSNIT curve for the elevation simulation is nearly symmetrical with respect to the Y axis within $\pm 15°$. M1 and M2 are still contributors for elevation angles less than $\pm 10°$, the same as the azimuth simulation.

As the elevation angle increases to +30°, rays can be scattered by M1 and the structure of the telescope. The PSNIT decreases slowly from +30° due to random scattering by the telescope, and the PSNIT value of elevation is about 1 to 2 orders of magnitude higher than the curve from the azimuth simulation. The input rays are perpendicular to the telescope at +90°, and only rays scattered by the dome will enter the light path.

For elevation angle between –10° and –15°, the rays scattered by M1 and the structure of the telescope dominate the total flux on the focal plane. The dome shutter will block rays from entering the telescope directly when elevation angle is larger than –15°, and the dome surface becomes the stray light contributor. Beyond –40°, when the stray light source comes to the back of the dome, all rays will be blocked.

5.3 Adding Vanes inside the Secondary Baffle

In optical astronomical telescopes, the vanes are usually located inside the primary baffle and the secondary baffle, blocking scattered light and improving the stray light performance.

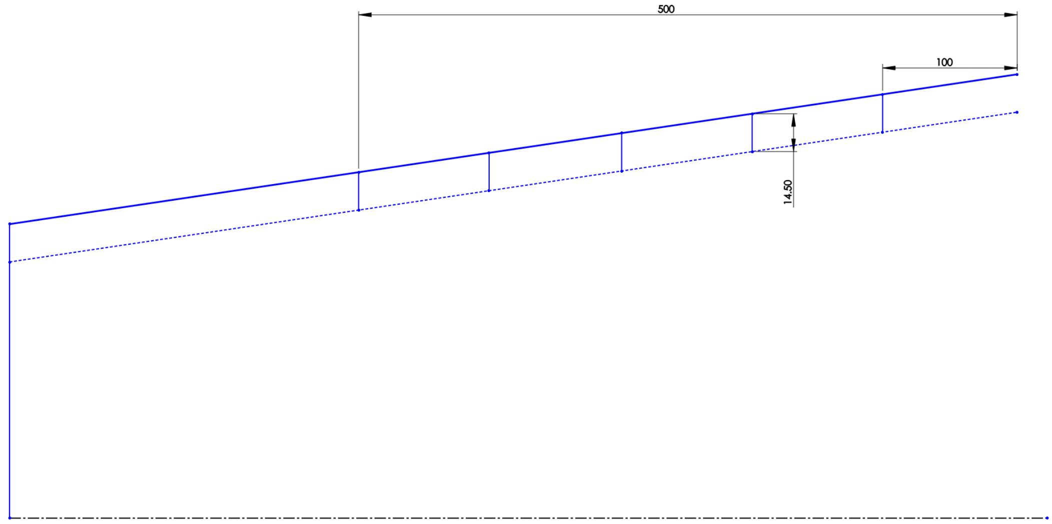

Fig. 12 Design for vanes in the M2 baffle of the Xinglong 2.16-m telescope (not to scale). The *solid* and *dotted lines* represent the profile of the M2 baffle and the marginal rays, respectively. The *dash-dotted line* is the optical axis. The five vanes located at the inner surface of M2 baffle every 100 mm from the bottom (*right side*). The depth of each vane is 14.5 mm in order to avoid blocking by marginal rays.

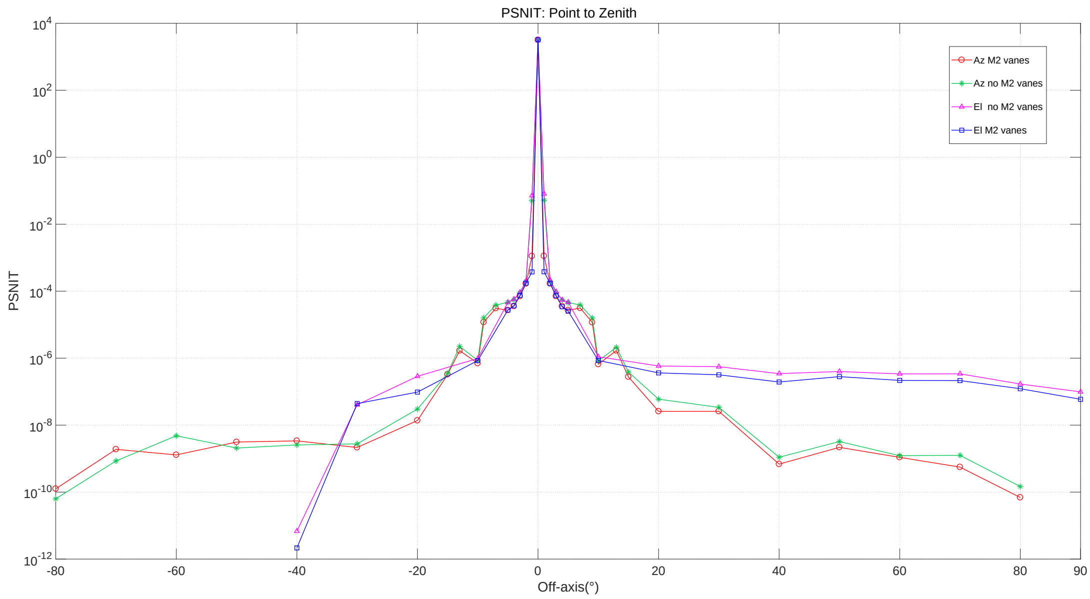

Fig. 13 PSNIT with/without vanes, telescope is pointed to zenith (predicted reduction in intensity of scattered light).

As a result of analyzing the "Ray Path Sorting" table for all angles, it is clear that almost all rays coming from the telescope structure (center section, mount ...) and dome will be scattered by the secondary baffle (M2 baffle) before arriving at the focal plane. Figure 11 shows the ray path for elevation angle +30° in the case "point to zenith." Considering the above conclusions, adding vanes inside the M2 baffle is a reasonable method for controlling stray light.

In Figure 12, the half profile of the M2 baffle is depicted (solid line), with marginal ray paths of the optical system indicated as a dotted line. For simplicity, this is shown not to scale and without optical components, and only the M2 baffle housing wall and the marginal rays are defined.

Based on the structure of the M2 baffle and the experiences of stray light control (the bottom part of the M2 baffle will block more scattered light), only five vanes perpendicular to the optical axis are utilized. The five vanes are located at the inner surface of the M2 baffle every 100 mm from the bottom. The depth of each vane is 14.5 mm in order to avoid blocking marginal rays.

Figure 13 displays the PSNIT results with or without vanes in azimuth and elevation when the telescope is pointed to zenith. It is clear that the vanes can improve the stray light performance in most cases, especially for a positive off-axis angle in both azimuth and elevation simulations. The downtrend of curves has not changed. The PSNIT values decrease about 40% on average.

The total number of rays is also reduced. As shown in Table 5, the total numbers of rays for azimuth and elevation simulations decrease by approximately eight-thousand and ten-thousand, respectively. In the elevation simulation, the suppression is more effective.

6 CONCLUSIONS

As one of the campaigns targeting stray light control for the Xinglong 2.16-m telescope, a detailed stray light analysis of the telescope is completed. The complex stray light simulations containing a simplified dome and telescope model are analyzed in two cases: "point to 60°" and "point to zenith." Identification of critical objects and illuminated objects, calculation of PSNIT curves and description of stray light contributors have been presented employing TracePro at different off-axis angles. In the future, a number of new instruments including spectrograph, tip-tilt and photopolarimeter will be available to the 2.16-m telescope, and stray light analysis of the 2.16-m telescope could provide an overview and significant guidance for improving instrument efficiency.

Acknowledgements Work described in this paper is supported by the National Natural Science Foundation of China (Grant No. 11703043) and Joint Research Fund in Astronomy, National Natural Science Foundation of China (No. U1831209). We thank Jin Ma and Yingwei Chen for providing details on the primary baffle of the 2.16-m telescope.

References

Bartell, F. O., Dereniak, E. L., & Wolfe, W. L. 1981, in Proc. SPIE, 257, Radiation Scattering in Optical Systems, ed. G. H. Hunt, 154
Bass, M., Stryland, E. W. V., Williams, D. R., & Wolfe, W. L. 2001, Handbook of Optics Volume III Classical Optics, Vision Optics, X-Ray Optics 2nd edition (New York: McGraw-Hill)
Bely, P. Y. 2003, The Design and Construction of Large Optical Telescopes (Berlin, New York: Springer)
Fan, Z., Wang, H., Jiang, X., et al. 2016, PASP, 128, 115005
Fest, E. C. 2013, Stray Light Analysis and Control (Washington USA: SPIE PRESS Bellingham)
Greynolds, A. W. 2007, in Proc. SPIE, 6675, Optical Modeling and Performance Predictions III, 66750B
Schaub M., Schwiegerling J., Fest E.C., 2011, Molded Optics: Design and Manufacture (Boca Raton: CRC Press)
Su, D.-Q. 2001, 2.16-m Telescope Work Collections (Beijing: Science and technology of China press)
TracePro, 2010, TracePro User's Manual Release 7.0 (Littleton:Lambda Research Corporation)